Available online at www.sciencedirect.com
ScienceDirect
Journal of Photochemistry and Photobiology A: Chemistry 182 (2006) 325–329
Journal of Photochemistry and Photobiology A:Chemistry
www.elsevier.com/locate/jphotochem

Self-alignment of Ge nano-particles in laser induced Bragg grating in Ge–B–SiO_2 film

Hiroaki Nishiyama [a,1], Junji Nishii [b,*]

[a] *Department of Manufacturing Science, Graduate School of Engineering, Osaka University, 2-1 Yamada-oka, Suita, Osaka 565-0871, Japan*
[b] *National Institute of Advanced Industrial Science and Technology, 1-8-31 Midorigaoka, Ikeda, Osaka 563-8577, Japan*

Abstract

Thermally stabilized photoinduced channel waveguides with Bragg gratings were fabricated in Ge–B–SiO_2 thin glass films using the site-selective precipitation technique of Ge nanoparticles. Refractive index of the film increased after annealing longer than 10 min at 600 °C. Such increase of refractive index seems to be responsible for the precipitation of Ge nanoparticles in the film. However, irradiation prior to annealing suppressed the increase of refractive index. Consequently, the annealing reversed the photoinduced refractive index pattern and also enhanced its thermal stability. The stabilized channel waveguide with a Bragg grating showed diffraction efficiency of 18.0 and 18.7 dB for TE- and TM-like modes, respectively. The diffraction efficiencies and wavelengths for both modes never changed after heat treatment at 500 °C, whereas the conventional photoinduced grating decayed even at 200 °C.

Keywords: Ge–B–SiO_2 thin glass films; Direct laser writing; Ge nanoparticles; Waveguides; Gratings

1. Introduction

Direct laser writing of micro-optical components in silica-based glasses is one of the promising processes for the realization of integrated optical circuits with fewer fabrication steps. The lithography and plasma etching processes have been used for the manufacturing of micro-optical components such as waveguides or gratings. Direct laser writing process, however, does not require such troublesome processes and thus much less expensive. So far, the fabrication of waveguides, gratings, directional waveguide coupler, waveguide laser, and so on has been reported [1–7]. However, thermal stability of the micro-optical components by direct laser writing is much lower than that by the conventional lithography and etching processes [8–12]. For example, thermal decay in a grating written in a Ge–B–SiO_2 core fiber using a pulse light source at 244 nm wavelength reportedly starts even at temperature below 150 °C [12]. Moreover, thermal stability of the grating written in a hydrogen loaded fiber is lower than that in nonloaded one [13,14]. Such thermal decay limits the application of devices fabricated by the direct laser writing.

We have reported an approach for thermally stabilized photoinduced refractive index changes in Ge–B–SiO_2 thin glass films [15–17]. A photoinduced grating in the film decayed remarkably after annealing at temperature below 500 °C. However, subsequent annealing at 600 °C reversed the photoinduced refractive index pattern of the photoinduced grating, yielding a new type of grating with high diffraction efficiency and thermal stability than that before annealing. We named such a grating, which is induced by the annealing, a thermally stabilized grating (TG). The origin of the TG is the periodic precipitation of crystalline Ge nanoparticles in the films. In this paper, we fabricated the thermally stabilized channel waveguide with TG by laser irradiation and successive annealing. No changes in diffraction efficiencies and diffraction wavelengths of the TG in the channel waveguide were observed after heat treatment up to 500 °C for 1 h.

2. Experimental

$15GeO_2$–$5B_2O_3$–$80SiO_2$ (mol%) thin glass films with SiO_2 upper cladding layers were deposited on silica glass substrates at 400 °C by the plasma-enhanced chemical vapor deposition

* Corresponding author. Tel.: +81 727 51 9543; fax: +81 727 51 9637.
E-mail addresses: hiroaki@mapse.eng.osaka-u.ac.jp (H. Nishiyama), junji.nishii@aist.go.jp (J. Nishii).
[1] Tel.: +81 6 6879 7535; fax: +81 6 6879 7570.

1010-6030/$ – see front matter © 2006 Elsevier B.V. All rights reserved.
doi:10.1016/j.jphotochem.2006.05.028

(PECVD) setup. Respective thickness of the Ge–B–SiO_2 and upper SiO_2 layers were approximately 4 and 1 μm. Liquid sources of $Si(OC_2H_5)_4$, $Ge(OCH_3)_4$, and $B(OC_2H_5)_3$ were used as raw materials for SiO_2, GeO_2, and B_2O_3, respectively. Vapors of source materials were introduced with oxygen gas into a chamber and then decomposed using oxygen plasma. The plasma was enhanced by a radio frequency of 13.56 MHz with 250 W. The inner pressure was 53 Pa. Chemical compositions of thin films were analyzed using electron probe microanalysis. The refractive index, thickness, and propagation loss were measured using the prism coupling method. Photoinduced grating with a period of 530 nm were formed by irradiation with KrF excimer laser of 248 nm wavelength through a phase mask at room temperature without hydrogen loading. The laser fluence and pulse number for the grating formation were fixed at 80 mJ/cm^2/pulse and 12,000 pulses, respectively. Thermal annealing was carried out in a tube furnace with a nitrogen atmosphere. Transmission spectra of channel waveguides were measured with an optical spectrum analyzer using a wavelength tunable laser diode as a light source. The incident beam was butt-coupled into the channel waveguides using a single-mode optical fiber with a numerical aperture of 0.15.

3. Results and discussion

3.1. Inversion of refractive index and its origin

Fig. 1 shows changes of refractive indices at 632.8 nm wavelength of the unirradiated film and the irradiated film against an annealing time at 600 °C. The irradiated film was prepared by homogeneously irradiation under the condition of laser fluence of 180 mJ/cm^2 and pulse number of 27,000. The photoinduced refractive index increase was as large as 3.1×10^{-3}. After annealing for 10 min, the photoinduced refractive index difference between both films remarkably decreased to 0.5×10^{-3} with accompanying reduction of the refractive indices of both films. Refractive indices of both films increased after annealing period longer than 10 min. However, the rate of the refractive index increase of the irradiated film was much lower than that of the unirradiated one. As a result, the refractive index of the unirradiated film became higher than that of the irradiated one after annealing for longer than 10 min, in contrast with the case before annealing. Irradiation with higher laser fluence decreased the rate of the refractive index increase more effectively. Such rate of refractive index increase also depended on the glass composition strongly. The refractive index difference between the films induced by annealing of period longer than 10 min never changed after further annealing at 500 °C. It has been considered that the Ge related oxygen deficient defects play an important role for the photoinduced refractive index changes in Ge doped SiO_2 [18,19]. Recently, it was reported from the studies on the photochemical reaction mechanism responsible for the photoinduced refractive index change that the Ge^{2+} center is likely the major Ge related oxygen deficient center responding to the high energy ultraviolet laser light [20,21]. We infer that high photosensitivity of Ge–B–SiO_2 thin film also resulted from the photoinduced structural changes of Ge^{2+} centers because Ge–SiO_2 and Ge–B–SiO_2 deposited by PECVD system used in this study contained the highly photoactive Ge^{2+} centers [22]. One cause for thermal decay in the photoinduced refractive index increases is the thermal excitation of the electrons that are trapped at defects during irradiation [9]. Many researchers reported similar changes of the photoinduced refractive index change in the fibers by annealing [8–12].

Fig. 2 shows the surface of the films with TG, which was induced by annealing of the photoinduced grating longer than 10 min at 600 °C. The observation was carried out after HF etching. The SiO_2 layer was completely removed prior to the observation, which was confirmed by the change in diffraction efficiency. Fig. 2 shows that 20–40-nm-diameter nanoparticles were precipitated periodically on the TG surface. The pitch of the periodic structure was identical with that of the photoinduced grating before annealing. We previously reported two experimental results on the TG [17]: (1) the nanoparticles were precipitated predominantly in the unirradiated region. Namely, irradiation with KrF excimer laser prior to annealing effectively suppressed the precipitation of nanoparticles. (2) From X-ray diffraction measurement, nanoparticles were cubic Ge crystals.

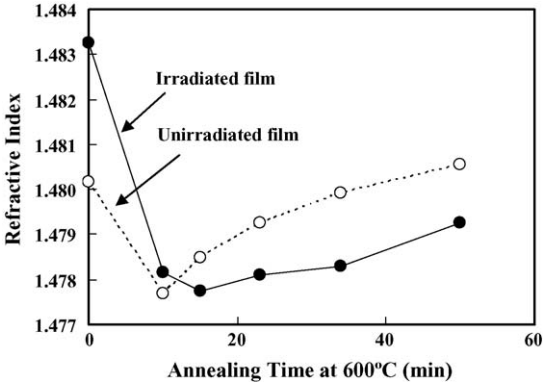

Fig. 1. Changes in refractive indices at 632.8 nm wavelength of the unirradiated film and the homogeneously irradiated film as a function of an annealing time at 600 °C. Irradiation was performed with KrF excimer laser under the condition of the photon density of 180 mJ/cm^2/pulse and shot number of 27,000.

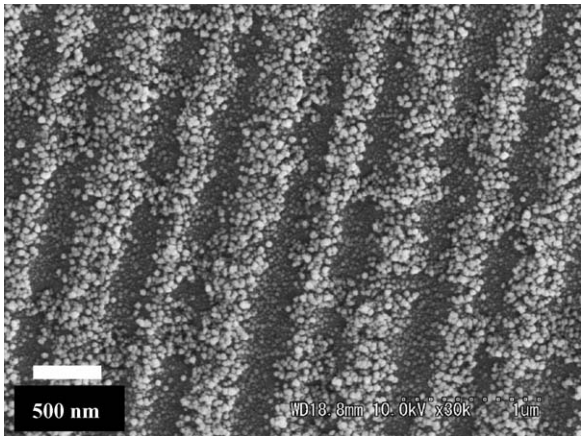

Fig. 2. SEM image of the TG surface after HF etching. Periodic precipitation of Ge nanoparticles was observed.

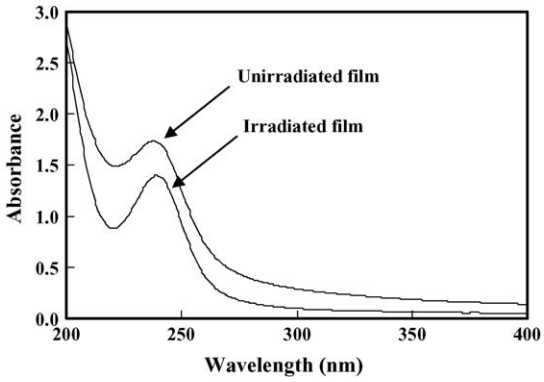

Fig. 3. Absorption spectra of the unirradiated film and the homogeneously irradiated film after annealing at 600 °C for 30 min.

We infer that the origin of the refractive index increases of both films after annealing period longer than 10 min is the precipitation of Ge nanoparticles because refractive index of Ge nanoparticles is considered to be much higher than that of oxide glasses. The lower rate of refractive index increase of the irradiated film than that of the unirradiated one can be understood by the suppression of Ge nanoparticles by irradiation prior to annealing.

Fig. 3 shows the absorption spectra of the unirradiated film and the irradiated one after annealing for 30 min. It is well known that the origin of the intense absorption peak around 236 nm is assignable to Ge related oxygen deficient defects [23]. It is apparent that the unirradiated film exhibited the larger absorption below 400 nm than the irradiated one. The absorption spectrum of the unirradiated film suggests the existence of Ge nanoparticles in the film. Kawamura et al. reported that similar absorption spectra were obtained as for the Ge–SiO_2 with Ge nanocrystals [24]. In addition, Wu et al. reported that the quantum confinement effect was observed by the measurements of absorption spectrum in the SiO_2 thin films with Ge nanocrystals prepared by RF-magnetron co-sputtering method [25]. According to their experimental results, as the diameter of the Ge nanocrystal decreases, the optical band gap shows remarkable blueshift relative to the bulk Ge. This size effect for optical band gap is consistent with the calculation [26]. Therefore, the absorption spectra in Fig. 3 suggest that the concentration of Ge nanoparticles in the unirradiated film was higher than that in the irradiated one, which is consistent with the experimental result that refractive index of the unirradiated film was higher than that of the irradiated one after annealing for 30 min in Fig. 1. Figs. 1 and 3 support the above inference that the origin of the refractive index increase after annealing was the precipitation of Ge nanoparticles. In Section 3.2, we tried to fabricate thermally stabilized channel waveguides with Bragg gratings by the site-selective precipitation technique of Ge nanoparticles.

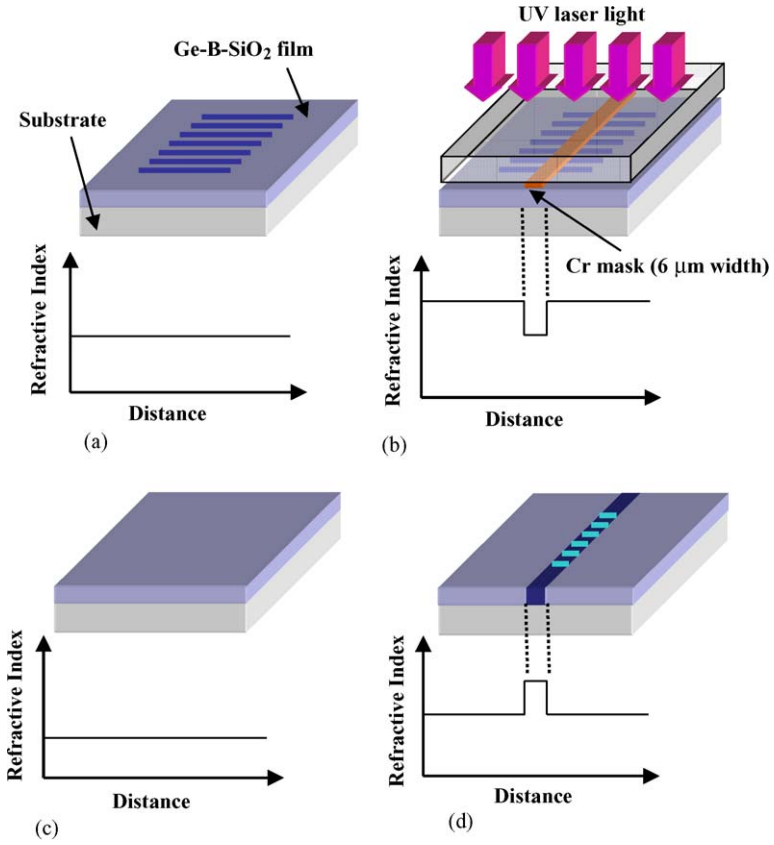

Fig. 4. Schematic fabrication processes of a thermally stabilized channel waveguide with TG by irradiation with KrF excimer laser and thermal annealing. The refractive index distributions in Ge–B–SiO_2 thin film at each process are also shown. (a) PG formation, (b) exposure through a Cr mask, (c) annealing at 600 °C for about 10 min, and (d) annealing at 600 °C for 20 min.

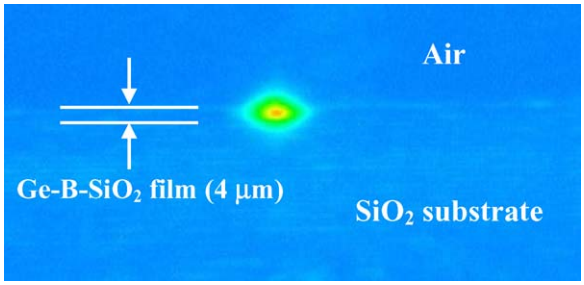

Fig. 5. Near-field pattern of the output beam from a thermally stabilized channel waveguide when the light of 1550 nm in wavelength was coupled. The height and width of the core were 4 and 6 μm, respectively.

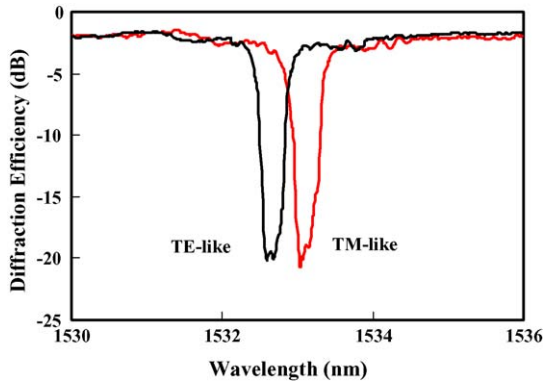

Fig. 6. Transmission spectra of a thermally stabilized channel waveguide with TG for TE- and TM-like modes. Diffraction peaks of 18.0 and 18.7 dB for TE- and TM-like modes were observed, which were located at 1532.7 and 1533.1 nm, respectively.

3.2. Direct laser writing of thermally stabilized channel waveguides with Bragg gratings

Thermally stabilized channel waveguides with TGs were fabricated using the site-selective precipitation technique. Fig. 4 schematically shows the fabrication processes and the expected refractive index distribution at each process. First, a 5-mm-long photoinduced grating was written in a thin film. Then, irradiation through a Cr mask with a straight line pattern of 6 μm width on a silica glass substrate was performed under the condition of the laser fluence of 180 mJ/cm^2/pulse and a pulse number of 27,000. Finally, this film was annealed at 600 °C for 20 min. These processes induced a channel waveguide structure with a 4-μm-high and 6-μm-wide core because annealing at 600 °C removed the photoinduced refractive index increase and then Ge nanoparticles with high refractive indices were predominantly precipitated in the unirradiated region. Annealing at 600 °C increased the propagation loss. The propagation loss of the film before and after annealing for 1 h was 0.4 and 1.4 dB/cm at 1545 nm wavelength, respectively. The increase in loss may be attributed to the precipitation of Ge nanoparticles.

Fig. 5 shows the near-field image of the output beam when the light at 1550 nm wavelength was coupled to the channel waveguide. The elliptical shapes of the output beam was mainly responsible for the asymmetrical core structure because the refractive index difference between core and cladding regions for the vertical direction was much larger than that for the in-plane direction. In addition, the anisotropic stresses in the channel waveguide may be one of the causes for the asymmetrical shape of the output beam. We infer from Fig. 1 that the refractive index difference between core and cladding regions for the in-plane direction was approximately 1.2×10^{-3} at 632.8 nm wavelength.

Fig. 6 shows the transmission spectra of the channel waveguide for TE- and TM-like modes. Diffraction peaks of 18.0 and 18.7 dB for the TE- and TM-like mode were clearly observed: they were located at 1532.7 and 1533.1 nm wavelength, respectively. These diffraction peaks indicate that annealing at 600 °C induced not only a channel structure, but also TG, which is the periodic structure consisting of Ge nanoparticles, in the film. Only one peak was observed for each polarization mode, meaning that a single-mode channel waveguide was induced. Polarization dependence of the diffraction peak positions is probably responsible for the asymmetrical core structure. It is considered that TG was induced only in the channel structure by annealing at 600 °C because the homogeneous irradiation in Fig. 4(b) was continued until the photoinduced grating in the cladding area was erased completely.

Fig. 7(a) and (b) shows changes in diffraction efficiencies and diffraction wavelengths, respectively, of the channel waveguide with TG after heat treatment up to 500 °C. Experimental results were also plotted for a photoinduced grating in a channel waveguide with $3GeO_2$–$11B_2O_3$–$86SiO_2$ (mol%) core and

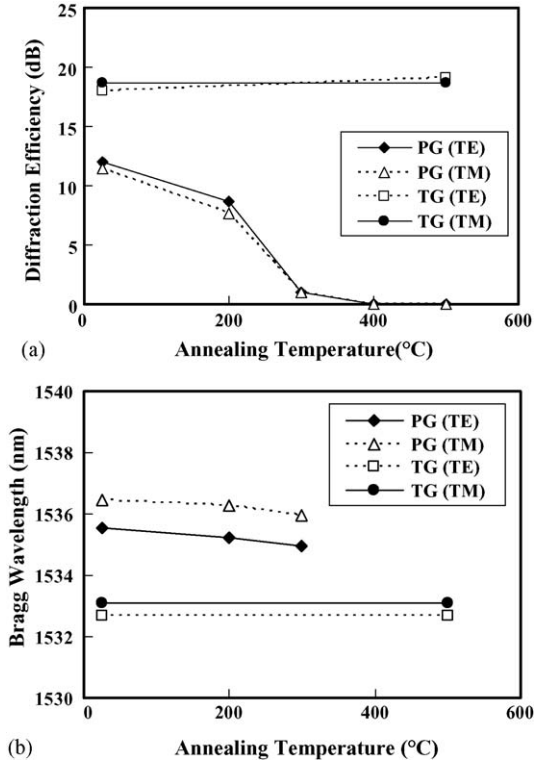

Fig. 7. Changes in (a) diffraction efficiencies and (b) diffraction wavelengths for TE- and TM-like modes of a thermally stabilized channel waveguide with TG after heat treatment up to 500 °C. For comparison, the experimental results for a channel waveguide with a PG are also plotted. Annealing time was 1 h at each temperature.

SiO_2 cladding fabricated by the photolithography and dry etching processes. The annealing time was 1 h at each temperature. Diffraction efficiencies for the photoinduced grating decreased and the peak positions exhibited the blueshift with temperature increase, which is resulted from thermal decay in photoinduced refractive index change [27]. In particular, the photoinduced grating was erased completely after heat treatment up to 400 °C. It is noteworthy that neither diffraction peaks nor diffraction wavelengths of the TG changed even after heat treatment up to 500 °C. So far, some researchers reported thermal stabilization techniques on photoinduced gratings in fibers with various core compositions [28,29]. Although such stabilization techniques enhance the thermal stability, the amplitude of photoinduced refractive index change became much lower than that before heat treatment. Therefore, the site-selective precipitation technique of Ge nanopaticles by the irradiation followed by annealing is an effective way to form a highly thermally stabilized photoinduced channel waveguide with a Bragg grating. Optimization of irradiation and annealing conditions will realize a channel waveguide with a grating with more intense confinement of the guided light, higher diffraction efficiency, and thermal stability.

4. Conclusions

Thermally stabilized photoinduced channel waveguides with Bragg gratings were fabricated using the site-selective precipitation technique. The stabilized waveguide with a grating showed diffraction efficiencies of 18.0 dB for the TE-like mode and 18.7 dB for the TM-like mode, respectively. No diffraction efficiencies and wavelengths changed after heat treatment up to 500 °C, whereas diffraction efficiencies of the conventional photoinduced grating decayed after heat treatment at temperature as low as 200 °C. Thermally stabilized photoinduced optical components should be applicable to optical devices such as sensors operating at high temperature.

References

[1] K.O. Hill, P.St.J. Russell, G. Meltz, A.M. Vengsarkar, J. Lightwave Technol. 15 (1997) 1261.
[2] D. Milanese, M. Ferraris, Y. Menke, M. Olivero, G. Perrone, C.B.E. Gawith, G. Brambilla, P.G.R. Smith, E.R. Taylor, Appl. Phys. Lett. 84 (2004) 3259.
[3] M. Takahashi, A. Sakoh, K. Ichii, Y. Tokuda, T. Yoko, Appl. Opt. 42 (2003) 4594.
[4] M. Olivero, M. Svalgaard, Opt. Express 13 (2005) 8390.
[5] M. Olivero, M. Svalgaard, Opt. Express 14 (2005) 162.
[6] M. Svalgaard, A. Harpøth, T. Rosbirk, Opt. Express 13 (2005) 5170.
[7] D.A. Guilhot, G.D. Emmerson, C.B.E. Gawith, S.P. Watts, D.P. Shepherd, R.B. Williams, P.G.R. Smith, Opt. Lett. 29 (2004) 947.
[8] A.M. Streltsov, N.F. Borrelli, J. Opt. Soc. Am. B 19 (2002) 2496.
[9] T. Erdogan, V. Mizrahi, P.J. Lemaire, D. Monroe, J. Appl. Phys. 76 (1994) 73.
[10] M. Lancry, P. Niay, S. Bailleux, M. Douay, C. Depecker, P. Cordier, I. Riant, Appl. Opt. 41 (2002) 7197.
[11] S.R. Baker, H.N. Rourke, V. Baker, D. Goodchild, J. Lightwave Technol. 15 (1997) 1470.
[12] M. Douay, W.X. Xie, T. Taunay, P. Bernage, P. Niay, P. Cordier, B. Poumellec, L. Dong, J.F. Bayon, H. Poignant, E. Delevaque, J. Lightwave Technol. 15 (1997) 1329.
[13] J. Rathje, M. Kristensen, J.E. Pedersen, J. Appl. Phys. 88 (2000) 1050.
[14] H. Patrick, S.L. Gilbert, A. Lidgard, M.D. Gallagher, J. Appl. Phys. 78 (1995) 2940.
[15] J. Nishii, K. Kintaka, H. Nishiyama, T. Sano, E. Ohmura, I. Miyamoto, Appl. Phys. Lett. 81 (2002) 2364.
[16] H. Nishiyama, K. Kintaka, J. Nishii, T. Sano, E. Ohmura, I. Miyamoto, Jpn. J. Appl. Phys. 42 (2003) 559.
[17] H. Nishiyama, I. Miyamoto, S. Matsumoto, M. Saito, K. Fukumi, K. Kintaka, J. Nishii, Appl. Phys. Lett. 85 (2004) 3734.
[18] J. Nishii, K. Fukumi, H. Yamanaka, K. Kawamura, H. Hosono, H. Kawazoe, Phys. Rev. B52 (1995) 1661.
[19] M. Takahashi, H. Shigemura, Y. Kawamoto, J. Nishii, T. Yoko, J. Non-Cryst. Solids 259 (1999) 149.
[20] M. Takahashi, K. Ichii, Y. Tokuda, T. Uchino, T. Yoko, J. Nishii, T. Fujiwara, J. Appl. Phys. 92 (2002) 3442.
[21] T. Uchino, M. Takahashi, T. Yoko, Phys. Rev. Lett. 84 (2000) 1475.
[22] A. Sakoh, M. Takahashi, T. Yoko, J. Nishii, H. Nishiyama, I. Miyamoto, Opt. Express 11 (2003) 2679.
[23] H. Hosono, Y. Abe, D.L. Kinser, R.A. Weeks, K. Muta, H. Kawazoe, Phys. Rev. B46 (1992) 11445.
[24] K. Kawamura, H. Hosono, H. Kawazoe, J. Appl. Phys. 80 (1996) 1357.
[25] X.M. Wu, M.J. Lu, W.G. Yao, Surf. Coat. Technol. 161 (2002) 92.
[26] T. Takagahara, K. Takeda, Phys. Rev. B46 (1992) 15578.
[27] B.O. Guan, H.Y. Tam, X.M. Tao, X.Y. Dong, IEEE Photon. Technol. Lett. 12 (2000) 1349.
[28] G. Brambilla, Appl. Phys. Lett. 81 (2002) 4151.
[29] Y. Shen, T. Sun, K.T.V. Grattan, M. Sun, Opt. Lett. 28 (2003) 2025.